

Fate Mapping and Transcript Profiling of Germinal Center Cells by Two-Photon Photoconversion

Imogen Moran and Tri Giang Phan

Abstract

The germinal center (GC) reaction is the key process for the generation of high affinity antibodies to foreign antigen. Standard experimental techniques such as fluorescence-activated cell sorting and histology have provided numerous insights into the composition and function of the GC. However, these approaches are limited to a “snapshot” in time and are unable to fully capture the dynamic nature of the GC. Intravital two-photon microscopy overcomes these disadvantages and has led to several major advances in the field but is restricted by practical and technical limits that prevent long-range mapping and molecular studies. Here we describe procedures for optical marking or “tagging” of cells in precise microanatomical compartments by two-photon photoconversion that can be used for long-term fate mapping and transcript profiling of GC T and B cells.

Key words Two-photon microscopy, Two-photon photoconversion, Fate mapping, Germinal center, Cell migration

1 Introduction

The germinal center (GC) is a transient structure that forms within the B cell follicle of secondary lymphoid organs where B cells undergo somatic hypermutation and antigen-based selection for BCR specificity and affinity [1, 2]. GCs were originally described by histology to consist of a proliferating dark zone (DZ) of centroblasts and nonproliferating light zone (LZ) of centrocytes. Within the LZ, GC B cells may interact with antigen trapped in the form of immune complexes on the surface of follicular dendritic cells (FDCs) that express high levels of complement and Fc receptors [1]. In the LZ, GC B cells may also interact with T follicular helper (Tfh) cells that provide critical cytokines and costimulatory molecules to support their differentiation, survival and growth [3]. In the classical model, GC B cells improve their affinity for antigen by repeatedly cycling between the DZ (where they proliferate and mutate their BCR), and the LZ (where they are selected to

differentiate into long-lived plasma cells or memory cells). GC B cells that fail to compete for antigen and T cell help, or have acquired self-reactivity undergo apoptosis and are phagocytosed by tingible body macrophages (TBMs) located at the junction between the DZ and LZ. However, this complex cellular dynamics within the GC has meant that traditional experimental techniques such as fluorescence activated cell sorting (FACS) and histology can only provide snapshots of the underlying cellular processes.

Intravital two-photon microscopy (TPM) has become the gold standard for minimally invasive imaging of cell migration and interactions deep inside intact organs of live animals [4, 5] and provided key insights into the major events in B cell activation in the humoral immune response [6]. Since the first landmark studies that visualized cycling of GC B cells between LZ and DZ [7–9], there has been much progress in our understanding of GC dynamics. Thus, CD169⁺ subcapsular sinus macrophages were shown to capture and present antigen to B cells to initiate the antibody response in the lymph node [10–14]. Activated B cells then relocalized to the T-B border and interfollicular zones where they interacted with T helper cells [15–17]. This interaction between T and B cells is dependent on the SLAM-associated protein (SAP) [18] and results in ICOS-mediated migration of Tfh cells [19] into the follicle and formation of the GC. Inside the GC, Tfh cells become “entangled” with GC B cells in multiple brief but extensive surface contacts [20, 21]. More recently, the migration pattern of primary [22, 23] and secondary Tfh cells [22, 24] have also been described.

Despite these advances, TPM does suffer from some practical limitations that make it difficult to achieve long-range fate mapping of cells over the course of the immune response [5]. In addition, while TPM is able to reveal dynamic changes in the location and behavior of the cells, it is unable to provide the molecular mechanisms that drive these changes. To overcome these limitations, investigators have developed strategies for *in vivo* optical marking (“tagging”) of cells in precise microanatomical locations using two-photon photoactivation of PA-GFP [25] and two-photon photoconversion (TPP) of Kaede [22, 26] and Kikume [27]. Optically marked cells can be tracked for long distances to distant organs following recovery of mice from anesthesia [26] and cells can be isolated for microarray [25] or single cell transcript analysis [22]. Our lab has focused on the Kaede system [28] because the cells are visible prior to irreversible photoconversion making it possible to image photoconverted (red) and non-photoconverted (green) cells in the same experiment. Furthermore, the photoconverted Kaede protein is more stable than photoactivated GFP with an estimated half-life of >1 week for Kaede [26] compared to 30 h for PA-GFP [25]. Antigen-specific B and T cell responses can thus be tracked by breeding Kaede mice with immunoglobulin knockin mice such the

SW_{HEL} mouse [29, 30] and TCR transgenic mice such as OT2 mouse [31]. This protocol describes the procedure of TPP for fate mapping and transcript profiling of germinal center T and B cells.

2 Materials

2.1 Mice

1. Kaede transgenic mice (*see Note 1*).
2. BCR knockin SW_{HEL} B cells and OT2 TCR transgenic CD4⁺ T cells (*see Note 2*).
3. SAP-deficient or wild-type mice as recipients (*see Note 3*).

2.2 Adoptive Cell Transfer

1. Dissecting instruments: dissecting scissors, forceps.
2. 2FD: 2% (v/v) fetal bovine serum in DMEM.
3. 15 mL polypropylene tubes (e.g., Falcon).
4. 50 mL polypropylene tubes (e.g., Falcon).
5. 1 mL syringe.
6. 70 μ m cell strainer.
7. RBC Lysis Buffer: 0.15 M ammonium chloride (NH₄Cl), 10 mM potassium hydrogen carbonate (KHCO₃), 0.1 mM sodium EDTA (Na₂EDTA) in Baxter water, pH 7.2–7.4.
8. Fetal calf serum (FCS).
9. MACs Buffer: 0.5% bovine serum albumin, 2 mM EDTA, 0.09% azide in PBS, filter sterilized.
10. Biotinylated anti-B220 clone RA3-6B2, anti-CD11b clone M1/70, anti-CD11c clone HL3, anti-CD43 clone S7.
11. MACS anti-biotin magnetic beads (Miltenyi).
12. LS columns (Miltenyi).
13. MACs Separator (Miltenyi).
14. Hemocytometer.
15. Trypan Blue.
16. 5 mL round bottom flow cytometry tubes.
17. Lysozyme from chicken egg white (e.g., Sigma).
18. Fc-block anti-CD16/32 clone 2.4G2.
19. Fluorochrome conjugated anti-B220, anti-CD4, anti-V α 2 antibodies.
20. HyHEL9 monoclonal antibody.
21. Alexa Fluor 647 Monoclonal Antibody Labeling Kit (Invitrogen) or equivalent.
22. Flow cytometer.
23. FlowJo or equivalent software to analyze flow cytometry data.
24. 0.5 mL insulin syringe for intravenous injection.

2.3 Immunization

1. Antigen for immunization, (*see Note 4*).
2. Albumin from chicken egg white (e.g., Sigma), for OVA immunization.
3. OVA_{323–339} peptide (CGGISQAVHAAHAEINEAGR), for conjugation to HEL to make HEL-OVA.
4. Succinimidyl-6-((β -maleimidopropionamido) [5] hexanoate) (SMPH), for HEL-OVA conjugation.
5. Lysozyme from chicken egg white (e.g., Sigma), for HEL-OVA immunization.
6. Sigma Adjuvant System (SAS).
7. 0.5 mL insulin syringe for subcutaneous injection.

**2.4 Labeling
Germinal Centers**

1. Anti-CD157 clone BP-3, (*see Note 5*).
2. Alexa Fluor 555, 647, and 680 labeling kit (Invitrogen) or CF680R kit (Biotium), (*see Note 6*).
3. 0.5-mL insulin syringe for subcutaneous injection.

**2.5 Preparation of
Mouse for Lymph Node
Imaging**

1. Anesthesia: Ketamine and xylazine diluted as described.
2. Bain circuit for gaseous anesthesia with isoflurane.
3. Custom Biotherm SmartStage (Cryologic).
4. Lacri-lube.
5. Electric razor.
6. Micropore Tape.
7. 70% ethanol.
8. Microdissecting Instruments: dissecting scissors, microscissors, forceps, sutures, needle holders.
9. Stereomicroscope.
10. Polydimethylsiloxane (PDMS) (e.g., Sylgard).
11. T-putty (Thermagon).
12. Vetbond tissue adhesive (3 M).
13. PBS.
14. Silicone grease.
15. Small O-ring.
16. Immersol Immersion Oil (Carl Zeiss).

**2.6 Two-Photon
Microscope**

1. Software-tunable ultrafast Near Infra-Red (NIR) Laser. We use a Chameleon Vision II ultrafast Ti:Sa laser (Coherent Scientific) The laser wavelength and dispersion compensation settings are controlled by the real-time computer, which also controls and synchronizes data acquisition by the microscope.
2. Two-photon microscope. We use an upright Zeiss 7MP two-photon microscope (Carl Zeiss) with a W Plan-Apochromat

20 \times /1.0 DIC (UV) Vis-IR water immersion objective. Four external non-descanned detectors are used to detect blue (SP-485), green (BP 500–550), and far-red (BP 640–710) emissions. We use the ZEN software interface to enable real-time interactive control of photoconversion parameters.

2.7 Two-Photon Photoconversion

1. Plastic coverslips.
2. Vicryl sutures.
3. Temgesic diluted as described.

2.8 Fluorescence-Activated Cell Sorting (FACS)

1. FACS analyzer for data acquisition, e.g., LSR II SORP or FACS Canto (BD).
2. FACS sorter for single cell sorting, e.g., FACS ARIA (BD).

3 Methods

An overall experimental timeline is shown in (Fig. 1) and example experimental results is shown in (Fig. 2).

3.1 Transfer Fluorescent Cells to Recipient Mice

3.1.1 Harvest Tissue Donor Mice

1. Euthanize fluorescent antigen-specific reporter mice, such as Kaede OT2 and tdTomato SW_{HEL} mice according to local ethical guidelines, (*see Note 7*).
2. Harvest spleen into 2 mL 2FD media in 15-mL tube. If additional donor cells are required also harvest inguinal, axillary and brachial lymph nodes

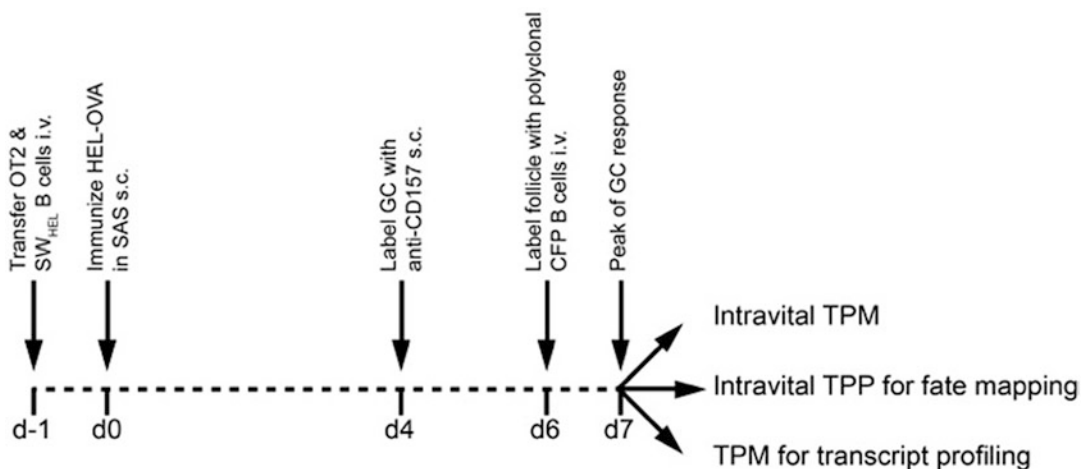


Fig. 1 Example experimental timeline for TPM or TPP of GCs in the inguinal lymph node. Fluorescent antigen-specific Kaede OT2 T cells and Tomato SW_{HEL} B cells are transferred into nonfluorescent recipient mice and immunized subcutaneously with antigen. The GC is labelled with fluorescently labeled anti-CD157 mAb injected 3 day before imaging, and the B cell follicle with polyclonal CFP B cells 1 day before imaging. GCs can then be imaged or photoconverted in the inguinal lymph node

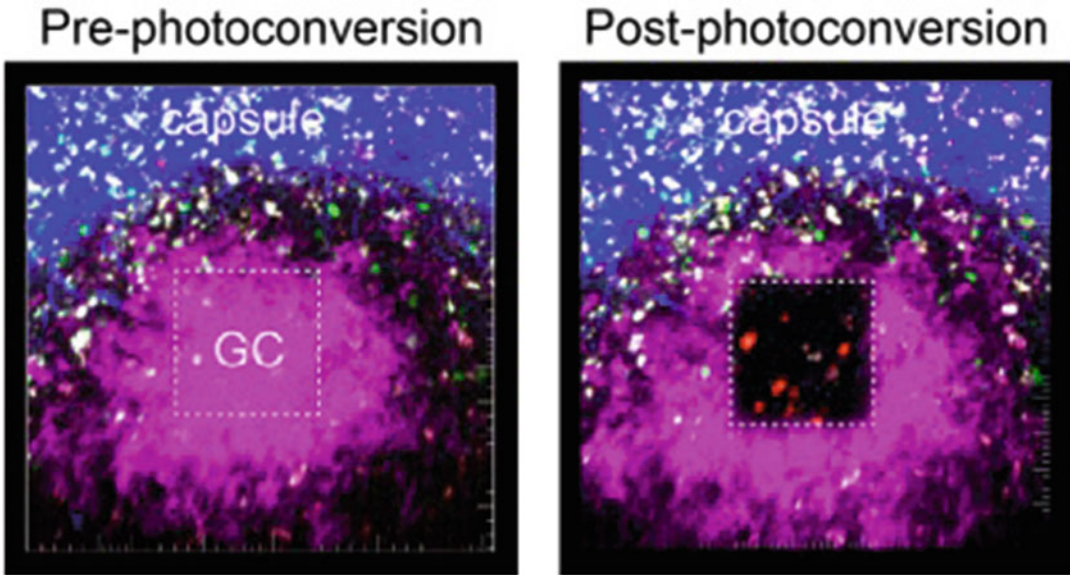


Fig. 2 Example of TPP of Tfh cells in the GC. Kaede OT2 T cells (*green*) were adoptively transferred into recipient mice and immunized with OVA in SAS. The GC was labeled by injection of anti-CD157 AF680 (*magenta*) on d4 and the follicle labeled by adoptive transfer of CFP B cells (*cyan*) on d6. Images of the draining inguinal lymph node were acquired on d7 (*left panel*) before TPP. The ROI (*dashed square*) targeted for photoconversion is shown. Images acquired following conversion (*right panel*) shows photobleaching of the GC label in the ROI which now contains photoconverted (*red*) Kaede OT2 T cells

3.1.2 Cell Preparation

All centrifugation steps for splenocytes in 50-mL tubes are performed at $453 \times g$ for 5 min at 4°C .

1. Prepare single cell suspension of splenocytes in 10 mL 2FD with $70\ \mu\text{m}$ cell strainer and 1 mL syringe plunger.
2. Lyse RBC in 5 mL RBC Lysis buffer and underlay with 1 mL FCS.
3. Centrifuge and resuspend cells in 10 mL MACs buffer.
4. Repeat procedure for lymph nodes, if harvested, without RBC lysis step. Spleen and lymph node cells can then be combined.
5. Count cells and resuspend at 10^8 cells/mL.
6. To enrich donor population of interest, we utilize negative selection with biotinylated antibodies. Cells are stained with the following biotinylated antibodies typically at $5\ \mu\text{g}/\text{mL}$ for 30 min on ice: To enrich for CD4 T cells in OT2 donor mice deplete with biotinylated anti-B220, anti-CD11b, anti-CD11c. To enrich for B cells in SW_{HEL} donor mice deplete with biotinylated anti-CD4, anti-CD11b, anti-CD11c, anti-CD43.
7. Wash cells twice in 10 mL MACs buffer

8. Resuspend cells at 10^8 cells/mL and stain with MACS anti-biotin magnetic beads for 30 min on ice. Wash cells twice in 10 mL MACs buffer.
9. Run filtered samples through MACs buffer prewashed LS columns on MACs Separator to isolate the negative fraction donor population of interest.
10. Determine the purity and yield of $CD4^+ V_{\alpha 2}^+$ OT2 population or $B220^+$ HEL-binding SW_{HEL} population by FACS analysis. Stain small volume of samples in FACS tube with following antibodies for 30 min on ice and wash twice in between staining steps at $453 \times g$ for 5 min. For OT2 T cell cells stain: anti-CD4 (fluorochrome labeled) + anti- $V_{\alpha 2}$ (fluorochrome labeled). For SW_{HEL} population stain cells: Fc-block (anti-CD16/32) + HEL (200 ng/mL). Anti-B220 (fluorochrome labeled) + HyHEL9 monoclonal antibody labeled with A647.
11. Count cells after enrichment and determine total number of donor cell population from purity analysis, (*see Note 8*).
12. Transfer cells to recipient mice. 2.5×10^5 $CD4^+ V_{\alpha 2}^+$ fluorescent OT2 T cells and, if using, 2.5×10^5 $B220^+$ HEL-binding fluorescent SW_{HEL} B cells were injected i.v. into age and sex matched recipient mice.

3.2 Immunizations

1. Immunize mice the day after cell transfer.
2. If transferred OT2 T cells immunize subcutaneously with 20 μ g of OVA in SAS in the lower flank and base of tail of mouse, (*see Note 9*)
3. If transferred both OT2 T cells and SW_{HEL} B cells, immunize subcutaneously with 20 μ g HEL-OVA in SAS.
4. Time to generate GCs will depend on antigen utilized but OVA and HEL-OVA responses in this system typically peak around 7 days after primary immunization.

3.3 Labeling FDCs in the GC LZ

1. Label anti-CD157 clone BP-3 with fluorescent protein labeling kit such as Alexa Fluor 680 or CF680R.
2. Inject 40 μ g fluorescent anti-CD157 s.c. on right hand imaging side of mouse in the lower flank and base of tail 3 days or more prior to imaging (*see Note 5*).

3.4 Labeling the B Cell Follicle

1. Isolate polyclonal B cells from different fluorescent donor color to transferred donor cells, as previously described in Subheading 3.1.
2. ~10 million injected i.v. 18–24 h prior to imaging.

3.5 Preparation of Mouse for Lymph Node Imaging

1. Induce anesthesia in the mouse with 100 mg/kg ketamine/ 5 mg/kg xylazine. Maintain anesthesia on 1–2% isoflurane supplemented with 100% oxygen.
2. Keep anesthetized mouse warm on a heating pad set to 37–38 °C.
3. Apply Lacri-Lube to eyes of mouse to prevent dryness.
4. Use an electric razor to shave hair on right flank and inguinal area. Use micropore tape to remove all hair from the area, (*see Note 10*).
5. Sterilize the skin with 70% ethanol and use sterile scissors to bluntly dissect a skin flap on the right hand side that exposes the inguinal lymph node and the inguinal ligament.
6. Apply T-putty to base of PDMS polymer (*see Note 11*) and stick to base of heating pad.
7. Stick skin flap, with skin to outside, down on PDMS, making sure the inguinal lymph node is in the middle of the PDMS not touching the VetBond glue.
8. Apply T-putty to seal the outside of skin flap. This will further fix the skin flap and also conduct heat from the heating pad.
9. Make a window in the skin overlying the inguinal lymph node using microscissors then apply PBS to keep the lymph node moist.
10. Carefully separate the lymph node from overlying fat and fascia layers to expose the cortical surface under a stereomicroscope with low-level illumination, (*see Note 12*).
11. Apply silicone grease to a small O-ring to adhere to skin around inguinal lymph node (*see Note 13*).
12. Put PBS in the O-ring to create a meniscus. Immersion oil may provide additional meniscus stability.

3.6 Two-Photon Microscopy

1. Transfer the mouse on heat pad to the microscope stage and reattach isoflurane nose cone to maintain anesthesia.
2. Set the microscope objective so that it is over the lymph node.
3. Tune the laser to the appropriate wavelength and adjust the power so that cells are visible, (*see Note 14*).
4. Set the upper and lower limits of the Z stack, typically 150 μm , and the number of images in the stack, typically step every 3 μm , (*see Note 15*).
5. Acquire image stacks at 30 s time intervals. Typically image for 30 min movies which is 60 cycles. Monitor drift and stop acquisition and check setup if large amount of drift is occurring.
6. Frequently monitor the mouse to check depth of anesthesia.

3.7 Real-Time Interactive Two- Photon Photoconversion for Fate Mapping

1. TPP is best performed with real-time interactive feedback to optimize the laser power and irradiation time for maximal photoconversion with minimal toxicity and photobleaching.
2. Locate cells of interest by scanning at 920 nm.
3. Set region of interest (ROI) to contain target cells. ROIs can be scaled from whole field of view down to single cell level by varying the laser power intensity (typically 20–60 mW) and duration of irradiation (typically 500–5000 cycles).
4. Tune laser to 840 nm and take a snap of the ROI. Note the mean pixel intensity in the green and red detectors. At 840 nm the Kaede green signal bleeds into the red channel.
5. Begin irradiating and note the changes in the mean pixel intensity in the green and red detectors. Initially the Kaede green signal and bleedthrough into the red channel will fall. Subsequently, the red signal will rise as Kaede is photoconverted. Adjust the laser power intensity if the green and red fluorescence is falling rapidly. Adjust stage position to correct for any lateral or axial shift during photoconversion.
6. Stop photoconverting when the green mean pixel intensity is less than half the original value and the rise in the red mean pixel intensity has plateaued, (*see Note 16*).
7. Determine the precision and level of photoconversion by scanning at 810 nm, (*see Note 17*).
8. Following photoconversion, clean and irrigate skin flap with PBS.
9. Suture skin window overlying the lymph node and close the skin flap with vicryl sutures.
10. Remove the mouse from the anesthetic machine and allow the mouse to recover from anesthesia on the heated stage (*see Note 18*).
11. Inject 75 $\mu\text{g}/\text{kg}$ temgesic s.c. as postoperative analgesia once mice show signs of waking.
12. Provide hydration and nutritional gel packs as necessary and monitor mice and the surgical wound closely in the first 4–8 h and daily thereafter. It is best to house mice singly post-op to prevent wound dehiscence.

3.8 Real-Time Interactive Two- Photon Photoconversion for Transcript Analysis

1. TPP can also be performed on ex plant lymph nodes for FACS phenotyping and transcript analysis. This has advantage over intravital TPP that the lymph node preparation is relatively fast and the procedure is high throughput. Also the explant tissue is kept at room temperature at which cells are less motile and this improves the precision and efficiency of the photoconversion.

2. Euthanize mice and harvest the lymph node by separating the fascia and fat overlying it in the inguinal ligament.
3. Clean the lymph node under the stereomicroscope. Make sure all fat and connective tissue is removed.
4. Use 20 μm pipette tip to apply very small amount of VetBond to plastic coverslip and mount the lymph node on the coverslip with cortical side up.
5. Remove any excess VetBond under the stereomicroscope.
6. Photoconvert as above in Subheading 3.7.
7. Following photoconversion, cells can be isolated and FACs phenotyped or sorted to examine their cellular or molecular characteristics.

3.9 Image Analysis

1. Import raw image files into Imaris (Bitplane) or similar image analysis software that allows 3D visualization of cells and semi-automated tracking.
2. Adjust image intensities and thresholds and apply smoothing function such as Gaussian filter used to reduce noise and improve contrast.
3. Drift correction is applied by utilizing stationary cells or landmarks.
4. Cells are detected using the spot detection function and tracks are then automatically generated which are then manually verified.
5. Surfaces and volumes can be applied to define structures such as the GC.
6. Motility parameters can be analyzed from the Imaris Statistics function such as average speed, arrest coefficient or displacement.

4 Notes

1. There are a number of genetically encoded fluorescent reporter mice that can be used for two-photon microscopy. We routinely use cyan fluorescent protein (CFP), green fluorescent protein (GFP), and tdTomato. For TPP we use Kaede transgenic mice crossed with SW_{HEL} (for B cells) or OT2 mice (for T cells). Kaede cells are green fluorescent and undergo photoconversion to red fluorescence on exposure to violet light or two-photon excitation with a NIR laser.
2. To examine antigen-specific and T and B cells in the GC, fluorescent reporter mice can be bred with SW_{HEL} (for B cells) or OT2 mice (for T cells). SW_{HEL} B cells recognize

hen-egg lysozyme (HEL) and OT2 CD4⁺ T cells recognize a peptide derived from ovalbumin (OVA).

3. We use SAP-deficient mice [32] as recipients. Endogenous SAP-deficient CD4⁺ T cells are less able to generate Tfh cells and this reduces competition with the adoptively transferred OT2 T cells.
4. HEL-OVA antigen is used when examining the response of both SW_{HEL} B cells and OT2 T cells. To prepare HEL-OVA, HEL protein is chemically conjugated to OVA peptide using the cross-linker SMPH as per the manufacturer's instructions. The HEL-OVA conjugation was checked by comparison to unconjugated HEL and a previous HEL-OVA conjugation on an SDS-PAGE gel with a Coomassie stain.
5. Several investigators have used different strategies for labeling the FDCs in the LZ of the GC such as fluorescent immune complexes and antigen. We have found that the anti-CD157 mAb BP-3 immediately labels the follicular stroma in resting lymph nodes but is redistributed to the GC after several days and labels the FDC network in immunized lymph nodes [22].
6. We have found that Alexa Fluor 647 rapidly bleaches compared to Alexa Fluor 680. More recently we have started using the CF680R labeling kits from Biotium and found them to be much more photostable for intravital imaging.
7. To examine Tfh cells only OT2 T cells are transferred and recipient mice immunized with OVA. To examine both Tfh and B cells, OT2 T cells and SW_{HEL} B cells are transferred and recipient mice immunized with HEL-OVA.
8. FACs purity is typically >80% for OT2 T cells and >97% for SW_{HEL} B cells.
9. It is important to warm the Sigma Adjuvant System for at least 30 min at 37 °C before use, typically in a water bath. After heating immediately mix the adjuvant 1:1 with OVA or HEL-OVA. Mix thoroughly and inject relatively quickly after preparation. Do not transport or store on ice.
10. It is necessary to remove as much hair as possible from the imaging area as hair is strongly autofluorescent.
11. We typically prepare the PDMS polymer in small petri dishes that can then be cut to an appropriate size and shape for the lymph node flap to sit on.
12. When exposing the lymph node it is important to be very careful to not disturb any of the blood vessels around the lymph node. A small capillary leak will obscure imaging from the hemoglobin in red blood cells. Also do not use bright light as this may inadvertently photoconvert the cells in the lymph node.

13. Silicone grease repels water so it is used both to stick the O-ring down to the skin flap and also to generate a hydrophobic barrier to help stabilize the meniscus.
14. Excitation wavelengths typically used are 810 nm (to optimally detect photoconverted Kaede red), 870 nm (to detect Alexa Fluor 555, Alexa Fluor 680, Kaede green), and 920 nm (to detect Kaede green, tdTomato). To save time we often reuse previous settings for different fluorescent proteins that give a rough guide of optimal settings for the current experiment.
15. Avoid oversampling by acquiring images at steps below the axial point-spread function and undersampling at steps larger than half the diameter of the cell of interest. Also avoid long time intervals as this will underestimate the instantaneous speed.
16. It is important to attenuate the laser power intensity correctly so that the cells are photoconverting without significant photobleaching. If the laser power is set too high it can result in photobleaching. High laser power can also be toxic to cells so it is important to check that TPP is nontoxic by comparing the migration velocities of the cells of interest both before and after photoconversion.
17. Photoconverted Kaede red is best detected at 810 nm. At 920 nm unphotoconverted Kaede bleeds into the red channel.
18. Anaesthetized mice are unable to maintain their body temperature and it is essential to keep mice warm at all times to improve surgical outcomes.

References

1. Allen CD, Okada T, Cyster JG (2007) Germinal-center organization and cellular dynamics. *Immunity* 27(2):190–202. doi:10.1016/j.immuni.2007.07.009
2. Victora GD, Nussenzweig MC (2012) Germinal centers. *Annu Rev Immunol* 30:429–457. doi:10.1146/annurev-immunol-020711-075032
3. Crotty S (2011) Follicular helper CD4 T cells (TFH). *Annu Rev Immunol* 29:621–663. doi:10.1146/annurev-immunol-031210-101400
4. Cahalan MD, Parker I (2008) Choreography of cell motility and interaction dynamics imaged by two-photon microscopy in lymphoid organs. *Annu Rev Immunol* 26:585–626. doi:10.1146/annurev.immunol.24.021605.090620
5. Phan TG, Bullen A (2010) Practical intravital two-photon microscopy for immunological research: faster, brighter, deeper. *Immunol Cell Biol* 88(4):438–444. doi:10.1038/icb.2009.116
6. Tangye SG, Brink R, Goodnow CC, Phan TG (2015) SnapShot: interactions between B cells and T cells. *Cell* 162(4):926–926 . doi:10.1016/j.cell.2015.07.055e921
7. Allen CD, Okada T, Tang HL, Cyster JG (2007) Imaging of germinal center selection events during affinity maturation. *Science* 315(5811):528–531. doi:10.1126/science.1136736
8. Schwickert TA, Lindquist RL, Shakhar G, Livshits G, Skokos D, Kosco-Vilbois MH, Dustin ML, Nussenzweig MC (2007) In vivo imaging of germinal centres reveals a dynamic open structure. *Nature* 446(7131):83–87. doi:10.1038/nature05573
9. Hauser AE, Junt T, Mempel TR, Sneddon MW, Kleinstein SH, Henrickson SE, von

- Andrian UH, Shlomchik MJ, Haberman AM (2007) Definition of germinal-center B cell migration in vivo reveals predominant intrazonal circulation patterns. *Immunity* 26 (5):655–667. doi:[10.1016/j.immuni.2007.04.008](https://doi.org/10.1016/j.immuni.2007.04.008)
10. Junt T, Moseman EA, Iannacone M, Massberg S, Lang PA, Boes M, Fink K, Henrickson SE, Shayakhmetov DM, Di Paolo NC, van Rooijen N, Mempel TR, Whelan SP, von Andrian UH (2007) Subcapsular sinus macrophages in lymph nodes clear lymph-borne viruses and present them to antiviral B cells. *Nature* 450 (7166):110–114. doi:[10.1038/nature06287](https://doi.org/10.1038/nature06287)
 11. Carrasco YR, Batista FD (2007) B cells acquire particulate antigen in a macrophage-rich area at the boundary between the follicle and the subcapsular sinus of the lymph node. *Immunity* 27 (1):160–171. doi:[10.1016/j.immuni.2007.06.007](https://doi.org/10.1016/j.immuni.2007.06.007)
 12. Phan TG, Grigorova I, Okada T, Cyster JG (2007) Subcapsular encounter and complement-dependent transport of immune complexes by lymph node B cells. *Nat Immunol* 8(9):992–1000. doi:[10.1038/ni1494](https://doi.org/10.1038/ni1494)
 13. Phan TG, Green JA, Gray EE, Xu Y, Cyster JG (2009) Immune complex relay by subcapsular sinus macrophages and noncognate B cells drives antibody affinity maturation. *Nat Immunol* 10(7):786–793. doi:[10.1038/ni.1745](https://doi.org/10.1038/ni.1745)
 14. Roozendaal R, Mempel TR, Pitcher LA, Gonzalez SF, Verschoor A, Mebius RE, von Andrian UH, Carroll MC (2009) Conduits mediate transport of low-molecular-weight antigen to lymph node follicles. *Immunity* 30 (2):264–276. doi:[10.1016/j.immuni.2008.12.014](https://doi.org/10.1016/j.immuni.2008.12.014)
 15. Okada T, Miller MJ, Parker I, Krummel MF, Neighbors M, Hartley SB, O'Garra A, Cahalan MD, Cyster JG (2005) Antigen-engaged B cells undergo chemotaxis toward the T zone and form motile conjugates with helper T cells. *PLoS Biol* 3(6):e150. doi:[10.1371/journal.pbio.0030150](https://doi.org/10.1371/journal.pbio.0030150)
 16. Kitano M, Moriyama S, Ando Y, Hikida M, Mori Y, Kurosaki T, Okada T (2011) Bcl6 protein expression shapes pre-germinal center B cell dynamics and follicular helper T cell heterogeneity. *Immunity* 34(6):961–972. doi:[10.1016/j.immuni.2011.03.025](https://doi.org/10.1016/j.immuni.2011.03.025)
 17. Kerfoot SM, Yaari G, Patel JR, Johnson KL, Gonzalez DG, Kleinstein SH, Haberman AM (2011) Germinal center B cell and T follicular helper cell development initiates in the interfollicular zone. *Immunity* 34(6):947–960. doi:[10.1016/j.immuni.2011.03.024](https://doi.org/10.1016/j.immuni.2011.03.024)
 18. Qi H, Cannons JL, Klauschen F, Schwartzberg PL, Germain RN (2008) SAP-controlled T-B cell interactions underlie germinal centre formation. *Nature* 455(7214):764–769. doi:[10.1038/nature07345](https://doi.org/10.1038/nature07345)
 19. Xu H, Li X, Liu D, Li J, Zhang X, Chen X, Hou S, Peng L, Xu C, Liu W, Zhang L, Qi H (2013) Follicular T-helper cell recruitment governed by bystander B cells and ICOS-driven motility. *Nature* 496(7446):523–527. doi:[10.1038/nature12058](https://doi.org/10.1038/nature12058)
 20. Liu D, Xu H, Shih C, Wan Z, Ma X, Ma W, Luo D, Qi H (2015) T-B-cell entanglement and ICOSL-driven feed-forward regulation of germinal centre reaction. *Nature* 517 (7533):214–218. doi:[10.1038/nature13803](https://doi.org/10.1038/nature13803)
 21. Shulman Z, Gitlin AD, Weinstein JS, Lainez B, Esplugues E, Flavell RA, Craft JE, Nussenzweig MC (2014) Dynamic signaling by T follicular helper cells during germinal center B cell selection. *Science* 345(6200):1058–1062. doi:[10.1126/science.1257861](https://doi.org/10.1126/science.1257861)
 22. Suan D, Nguyen A, Moran I, Bourne K, Hermes JR, Arshi M, Hampton HR, Tomura M, Miwa Y, Kelleher AD, Kaplan W, Deenick EK, Tangye SG, Brink R, Chtanova T, Phan TG (2015) T follicular helper cells have distinct modes of migration and molecular signatures in naive and memory immune responses. *Immunity* 42(4):704–718. doi:[10.1016/j.immuni.2015.03.002](https://doi.org/10.1016/j.immuni.2015.03.002)
 23. Moriyama S, Takahashi N, Green JA, Hori S, Kubo M, Cyster JG, Okada T (2014) Sphingosine-1-phosphate receptor 2 is critical for follicular helper T cell retention in germinal centers. *J Exp Med* 211(7):1297–1305. doi:[10.1084/jem.20131666](https://doi.org/10.1084/jem.20131666)
 24. Shulman Z, Gitlin AD, Targ S, Jankovic M, Pasqual G, Nussenzweig MC, Victora GD (2013) T follicular helper cell dynamics in germinal centers. *Science* 341(6146):673–677. doi:[10.1126/science.1241680](https://doi.org/10.1126/science.1241680)
 25. Victora GD, Schwickert TA, Fooksman DR, Kamphorst AO, Meyer-Hermann M, Dustin ML, Nussenzweig MC (2010) Germinal center dynamics revealed by multiphoton microscopy with a photoactivatable fluorescent reporter. *Cell* 143(4):592–605. doi:[10.1016/j.cell.2010.10.032](https://doi.org/10.1016/j.cell.2010.10.032)
 26. Chtanova T, Hampton HR, Waterhouse LA, Wood K, Tomura M, Miwa Y, Mackay CR, Brink R, Phan TG (2014) Real-time interactive two-photon photoconversion of recirculating lymphocytes for discontinuous cell tracking in live adult mice. *J Biophotonics* 7(6):425–433. doi:[10.1002/jbio.201200175](https://doi.org/10.1002/jbio.201200175)
 27. Suan D, Hampton HR, Tomura M, Kanagawa O, Chtanova T, Phan TG (2013) Optimizing fluorescence excitation and detection for intravital two-photon microscopy. *Methods Cell*

- Biol 113:311–323. doi:[10.1016/B978-0-12-407239-8.00014-8](https://doi.org/10.1016/B978-0-12-407239-8.00014-8)
28. Tomura M, Yoshida N, Tanaka J, Karasawa S, Miwa Y, Miyawaki A, Kanagawa O (2008) Monitoring cellular movement in vivo with photoconvertible fluorescence protein “Kaede” transgenic mice. *Proc Natl Acad Sci U S A* 105(31):10871–10876. doi:[10.1073/pnas.0802278105](https://doi.org/10.1073/pnas.0802278105)
 29. Phan TG, Amesbury M, Gardam S, Crosbie J, Hasbold J, Hodgkin PD, Basten A, Brink R (2003) B cell receptor-independent stimuli trigger immunoglobulin (Ig) class switch recombination and production of IgG autoantibodies by anergic self-reactive B cells. *J Exp Med* 197(7):845–860. doi:[10.1084/jem.20022144](https://doi.org/10.1084/jem.20022144)
 30. Brink R, Paus D, Bourne K, Hermes JR, Gardam S, Phan TG, Chan TD (2015) The SW (HEL) system for high-resolution analysis of in vivo antigen-specific T-dependent B cell responses. *Methods Mol Biol* 1291:103–123. doi:[10.1007/978-1-4939-2498-1_9](https://doi.org/10.1007/978-1-4939-2498-1_9)
 31. Barnden MJ, Allison J, Heath WR, Carbone FR (1998) Defective TCR expression in transgenic mice constructed using cDNA-based alpha- and beta-chain genes under the control of heterologous regulatory elements. *Immunol Cell Biol* 76(1):34–40. doi:[10.1046/j.1440-1711.1998.00709.x](https://doi.org/10.1046/j.1440-1711.1998.00709.x)
 32. Czar MJ, Kersh EN, Mijares LA, Lanier G, Lewis J, Yap G, Chen A, Sher A, Duckett CS, Ahmed R, Schwartzberg PL (2001) Altered lymphocyte responses and cytokine production in mice deficient in the X-linked lymphoproliferative disease gene SH2D1A/DSHP/SAP. *Proc Natl Acad Sci U S A* 98(13):7449–7454. doi:[10.1073/pnas.131193098](https://doi.org/10.1073/pnas.131193098)